ISSN 2070-0504, Catalysis in Industry, 2022, Vol. 14, No. 1, pp. 42–55. © Pleiades Publishing, Ltd., 2022.
Russian Text © The Author(s), 2021, published in Kataliz v Promyshlennosti.

CATALYSIS IN CHEMICAL AND PETROCHEMICAL INDUSTRY

Conversion of Methanol to Olefins: State-of-the-Art and Prospects for Development

R. V. Brovko[a], *, M. G. Sul'man[a], **, N. V. Lakina[a], *, and V. Yu. Doluda[a], ******

[a] *Tver' State Technical University, Tver', 170026 Russia*

**e-mail: RomanVictorovich69@mail.ru*

***e-mail: sulman@online.tver.ru*

****e-mail: lakina@yandex.ru*

*****e-mail: doludav@yandex.ru*

Received June 1, 2021; revised July 14, 2021; accepted July 16, 2021

Abstract—The production of olefins via the catalytic conversion of methanol on zeolites and zeotypes is of great interest to both the scientific community and specialists in related areas of the national economy. Due to the gradual industrial implementation of the above process, the focus of attention is gradually shifting from scientific research devoted to the synthesis and modification of zeolites and zeotypes of different structures; to studies of pilot and industrial installations; to determining the main economic and environmental indicators, both existing and planned; and to the construction of production facilities. In 2019 alone, China licensed the construction of 26 production sites with a capacity of 14 million t/yr for ethylene and propylene, and commissioned 14 enterprises with a total capacity of 7.67 million t/yr for ethylene and propylene. The established production facilities include a full cycle of coal processing that consists of coal gasification units for the production of synthesis gas; units for the production and purification of methanol and olefins; and units for the production of polyethylene and polypropylene. The total productivity of the commissioned plants is more than 21 million t/yr for ethylene and propylene. This work reviews sources published in the foreign literature over the past five years on the preparation and modification of catalysts, along with technological, economic, and environmental aspects of the production of olefins from methanol.

Keywords: olefins, methanol, catalytic conversion of methanol, zeolites, zeotypes

DOI: 10.1134/S2070050422010032

INTRODUCTION

The catalytic conversion of methanol on zeolites and zeotypes is a growing technology for the production of olefins that could largely supplant the traditionally used means of their production. Over the last five years, there has been a considerable rise in applied, theoretical, and scientific research in this area, accompanied by a substantial increase in the number of commissioned industrial installations. Twenty-six production facilities have been built or are now being planned in China alone. These include plants for coal gasification to produce syngas, the synthesis of methanol, the catalytic conversion of methanol into olefins, and the stages of polyethylene and polypropylene production. The total productivity of enterprises under construction alone will be 14 million t/yr for ethylene and propylene. The planned introduction of quotas for carbon dioxide emissions by the oil refining and chemical industries is also raising interest in the catalytic conversion of methanol into olefins, since it can be done with intial compounds obtained from bio-renewable sources. The aim of this work is therefore to give an overview of sources related to the scientific, technological, economic, and environmental aspects of producing olefins from methanol that have been published in foreign sources over the last five years.

HISTORY OF THE COMMERCIAL PRODUCTION OF OLEFINS FROM METHANOL

In the 1980s, scientific research conducted by Union Carbide (United States) led to the creation of silicoaluminophosphate (SAPO) molecular sieves, some of which (particularly SAPO-34 with a chabazite (CHA) structure) were highly active in the catalytic conversion of methanol to ethylene and propylene [1, 2]. Structural features of the SAPO-34 zeotype impose considerable restrictions on the formation of branched hydrocarbons, contributing to the high selectivity of the catalytic conversion of methanol into ethylene and propylene.

UOP and Norsk Hydro have jointly developed and demonstrated a new process of olefin synthesis using a

Table 1. Industrially Introduced Technologies for the Production of Olefins [9]

Technology	Operator	Performance, millions of t/yr	Catalyst	Process conditions	Technological indicators of the catalyst (conversion, %; selectivity, %)
UOP/Hydro	UOP (Feluy, Belgium)	0.2	SAPO-34	400–550°C 1–4 atm	100; 80
D-MTO	Shenhua China Energy	0.6	SAPO-34	400–550°C 4–5 atm	—
S-MTO	Sinopec	0.2	SAPO-34	400–550°C 1–5 atm	—
MTP (Lurgi)	Shenhua Group	0.5	SAPO-34	—	—
	Datang Int'l Power	0.5	SAPO-34	—	—
Honeywell UOP	Jiangsu Sailboat Petrochemical company	0.8	SAPO-34	400–550°C 1–5 atm	100; 85
	Wison China Energy	0.3	SAPO-34	400–550°C 1–5 atm	100; 85

catalyst containing the SAPO-34 zeotype that ensures up to 80% yields of ethylene and propylene with the near complete conversion of methanol [3]. The possibility of using synthesized olefins in the production of polyethylene and polypropylene was also evaluated in developing this process. The first demonstration plant for producing olefins from methanol used a fluidized bed reactor. This had several advantages, including the ability to continuously regenerate the catalyst. The moving bed of catalyst allowed a portion of the used catalyst to be continuously directed to a regenerator to remove coke deposits by combustion in air. It was therefore possible to maintain constant catalyst activity in the selected fluidized bed reactor, which ensured consistent composition of the product. However, it should be noted that a fluidized bed reactor has a lower specific capacity per unit volume, compared to a fixed bed reactor. Work done at a pilot plant in Porsgrun (Norway) confirmed the stability of the demonstration unit with a fluidized bed reactor over 90 days. The fluidized bed reactor also provided better heat recovery from the exothermic methanol-to-olefin conversion reaction [4].

The UOP/HYDRO process provides a fair degree of flexibility in the ratio of ethylene to propylene by allowing the process parameters of a plant's operation to be adjusted and the use of reactors with different capacities. The yield of carbon can be as 80%. Due to the formation of a complex mixture of hydrocarbons, however, the separation and purification of ethylene and propylene is required, raising the cost of olefins [4]. The subsequent development of this technology saw the introduction of an additional stage of cracking the formed hydrocarbons and improving the operational properties of the catalyst that is used. This raised the yield of olefins to 90% [5]. At the same time, the complete UOP/HYDRO production chain included the steam reforming of natural gas; the synthesis of methanol; the production, separation, and purification of of olefins; and the production of polypropylene and polyethylene [6]. It was planned to launch industrial plants for the production of olefins in Europe and Nigeria [7, 8], but economic difficulties allowed only the constriction of one plant in Belgium [9]. The UOP/HYDRO technology was subsequently revised slightly in China, with allowance for the lack of large reserves of natural gas. This required the stage of synthesis gas production to transition to the use of coal, which in turn raised the cost of the final product because of the greater technical complexity of the steam gasification of coal [9]. As a result, several similar technologies for the production of olefins were implemented in China (Table 1).

CATALYSTS

Improving current ways of synthesizing zeolites and zeotypes has in recent years become a trend in the development of catalysis by aluminosilicates, including the catalytic conversion of methanol into olefins. One of the main lines of development in this area is the synthesis of homogeneous nano- and microsized zeolites [10]. Reducing the size of zeolite and zeotype crystals helps lower the inhibition of diffusion and thus contributes to an increase in the process's selectivity toward ethylene [10, 11]. The authors of [10] described the synthesis of monodisperse nanoparticles of SAPO-34 zeotype using morpholine to control the particle size, while monodisperse cubic microparticles 4 μm in size were obtained. Adding morpholine as a modifier also helped reduce the number of strong acid sites responsible for the formation of aromatic and polyaromatic compounds. The selectivity of the catalytic conversion of methanol into ethylene and propyl-

ene rose from 40 to 45% and 37 to 45%, respectively (T = 425°C, WHSV = 2 h^{-1}). A more than 200% reduction in the rate of zeolite deactivation was also noted.

Nanostructured zeolite H-ZSM-5 [11, 12] with individual crystals 50–100 nm in size [11] showed higher selectivity toward light olefins C_2–C_4 than macrocrystalline samples. The highest selectivity (82.7% for light C_2–C_4 olefins) was obtained by reducing inhibitions to the diffusion of zeolite nanocrystals, relative to macrocrystalline samples (T = 490°C, WHSV = 1 h^{-1}) [11, 12].

The problems of growing zeotypes on different heterogeneous substrates are of considerable interest in preparing supported catalysts [13]. Zeotype SAPO-34 [13] was grown on surfaces of zirconium oxide, which is widely used as a support for catalytically active metals. The specific activity of SAPO-34 was not appreciably reduced, relative to free SAPO-34. However, operational lifetime grew by more than 70%, due to reduced acidity of the strong Brønsted sites of the modified zeolite.

The preparation of polystructural zeolites is another possible way of increasing the activity of a catalyst and the selectivity of methanol conversion to olefins [14]. The hydrothermal synthesis of mixed zeotypes with RHO and CHA structures was described in [14], where samples with 52 and 79% of the RHO phase and 48 and 21% of the CHA phase were obtained. Increasing the content of chabazite (CHA) raised the selectivity of methanol conversion to ethylene. Increasing the proportion of the RHO phase helped slow the rate of zeolite deactivation. The sample with 79% of the RHO phase showed no loss of activity after six consecutive cycles of use with intermediate oxidative regeneration in air flow.

Another area of constant interest to researchers is developing template-free methods for the synthesis of zeolites intended for use in the catalytic conversion of methanol into olefins and other processes [15]. The authors of [15] studied the template-free synthesis of chabazite (Table 2) and the of crystallization and the period of aging on the crystallinity of chabazite. It was shown that 120 h of crystallization is sufficient for the formation of chabazite with a micropore volume of 0.19 cm^3/g and a mesopore volume of 0.02 cm^3/g. The synthesized chabazite displayed high selectivity toward ethylene (up to 60%), while the selectivity of the process toward propylene was 20%.

Ways of synthesizing zeolites and zeotypes with different structures continue to be developed for the targeted production of mostly individual components (ethylene or propylene) (see Table 2). One way of increase the selectivity toward light olefins is introducing heteroatoms in order to modify the acidic properties of zeolites. The authors of [16] described the synthesis of boron-containing nanocrystalline zeolite (see Table 2) using 6-diaminohexane (6DH) and cytyltriethylammonium bromide (CTMABr) as structure-forming agents and boric acid as the source of boron. The synthesized sample of mesoporous zeolite H-ZSM-5 had a micropore volume of 0.092 cm^3/g, a mesopore volume of 0.081 cm^3/g, a Si : B ratio of 102, and 42% selectivity toward propylene.

The synthesis and study of gallium-containing zeolite H-ZSM-5 during the catalytic conversion of methanol with the production of olefins were covered in [17, 18]. The most active sample (see Table 2) was characterized by a low micropore volume of 0.06 cm^3/g. The volume of mesopores was twice as large at 0.13 cm^3/g. The maximum achieved selectivity toward ethylene was 23%, while the selectivity toward propylene was 27%. The increase in the selectivity of gallium-modified zeolite toward ethylene and propylene relative to the initial H-ZSM-5 can be attributed to both the modifying effect of gallium itself and a drop in the total acidity of active sites.

The synthesis of a gallium-containing zeolite sample with a CON-type structure using N,N,N-trimethyl-(–)-cis-hydroxymertanylammonium (TMHM) as a structure-forming agent was described in [19]. The most active sample [Ga, Al, B]-CON (250) (see Table 2) was characterized by a micropore volume of 0.235 cm^3/g. The number of available acid sites was greater than in other samples at 0.067 mmol/g. The achieved propylene selectivity was 52%, while the selectivity toward ethylene was only 5% at a methanol WHSV of 0.2 h^{-1}.

Introducing zinc into the SAPO-34 zeotype [20] contributed to a considerable increase in the selectivity of the process toward ethylene, from 35–40 to 50–53%. However, a parallel increase in the rate of zeolite deactivation was also observed. It was assumed there were Zn particles both in the mouths of the pores of SAPO-34 zeolite and on its outer surface. The increase in the yield of ethylene was thus a result of secondary reactions occurring on zinc surfaces.

The preparation of titanium-containing zeotype SAPO-34 with an average crystallite size of 100 nm was described in [21] along with its catalytic properties in the synthesis of olefins. Cubic zeotype nanoparticles were obtained via standard hydrothermal synthesis using tetroethyl ammonium hydroxide as a structure-forming agent. The results for the chemisorption of ammonia showed that including Ti in the zeotype increased the concentration of acid sites, which helped raise its catalytic activity and selectivity toward light olefins (from 60 to 80%).

The synthesis of phosphorus-containing chabazite and the study of its catalytic properties were described in [22]. Trimethyladamantyl ammonium hydrochloride (TMAHA) was used as the structure-forming agent, and tetraethyl phosphonium hydroxide served as the source of phosphorus (see Table 2). The highest selectivity toward ethylene (24%) was achieved for the P-CHA sample (0.44). The volume of micropores in

Table 2. Physicochemical and Catalytic Properties of Zeolites and Zeotypes in the Synthesis of Olefins

Sample	Synthesis	Si : Me	T, °C	WHSV, h^{-1}	S_{et}, %	S_{prop}, %	Reference
[Al]-[B]-ZSM-5	Na_2O = 0.01, Al_2O_3 = 0.005, H_3BO_3= 0.01, SiO_2 = 1, 6DG = 0.14, CTMABr = 0.1	Si : Al = 72, Si : B = 102	450	5.5	10	42	[16]
Sn-ZSM-5	SnO_2 = 0.01, Al_2O_3 = 0.003, SiO_2 = 1, TPGA = 0.25	Si : Al = 91, Si : Sn = 117	450	5	2.3	36	[25]
Ga-ZSM-5	Na_2O = 1250, Ga_2O_3 = 100, Al_2O_3 = 100, SiO_2 = 6, TPGA = 650	Si : Al = 156, Si : Ga = 28	320	10	23	27	[17, 18]
[Ga, Al, B] -CON (250)	H_3BO_4 = 0.1, Ga $(NO_3)_3$ = 0.004, Al_2O_3 = 0.0015, SiO_2 = 1, NaOH = 0.2, TMGM = 0.2	Si : Al = 402, Si : Ga = 0.62 Si : B = 21	500	0.2	5	52	[19]
Ag-SAPO-34	Al_2O_3 = 1, P_2O_5 = 1, SiO_2 = 0.4, TAGA = 2, AgPW = 0.01	Si : Al = 0.18, Si : Ag = 40	450	4	50	41	[26]
Zn-SAPO-34	Al_2O_3 = 0.43, P_2O_5 = 0.3, SiO_2 = 0.16, ZnO = 0.025	Si : Al = 0.2, Si : P = 0.25	500	10	53	25	[20]
CSSAPO-34-3	Al_2O_3 = 1, P_2O_5 = 1.5, SAPO-34 = 9, TEGA = 0.2, TEA = 2	Si : Al = 0.28, Si : P = 0.39	400	2	35	42	[27]
P-CHA (0.44)	Na_2O = 0.05, Al_2O_3 = 0.031, SiO_2 = 1, TEGP = 0.27, TMAGA = 0.3	Si : Al = 9.9 Si : P = 0.44	350	0.94	24	32	[22]
Al-CHA	K_2O = 0.39, Al_2O_3 = 0.2, SiO_2 = 1, NH_4F = 0.3	Si : Al = 2.5	400	0.95	60	20	[15]

this sample was 0.28 cm^3/g, and the Si : P ratio was <0.44.

Developing ways of intensifying the crystallization of zeolites is an important scientific and technical task that ensures a lower cost of zeolites. One way of reducing the period of crystallization is ultrasonic treatment of the reaction solution in order to increase the number of crystallization centers and raise the rate of zeolite crystal growth [23]. Synthesizing zeotype SAPO-34 [23] under the effects of ultrasound during crystallization helped raise the volume of zeotype micropores from 0.12 to 0.17 cm^3/g and reduce the period of crystallization to 5 h. The selectivity toward ethylene was 36% ($T = 450°C$, WHSV = 4.5 h^{-1}).

Another way of intensifying the formation of zeolite crystals is high-temperature hydrothermal synthesis [24]. Raising the temperature of hydrothermal synthesis to 350°C when obtaining zeolite H-ZSM-5 [24] helps reduce the period of crystallization to 0.5 h, and the resulting sample is characterized by 100% crystallinity. The selectivity of the catalytic methanol conversion to olefins on H-ZSM-5 samples synthesized in this way was 14% for ethylene and 80% for propylene ($T = 400°C$, WHSV = 2.9 h^{-1}), which corresponds to values obtained for samples synthesized with traditional hydrothermal treatment.

The study and synthesis of zeolites containing metal nanoparticles are of constant interest, due to the possibilities of regulating the acid-base properties of zeolites and introducing additional reactions into the chain of chemical conversions [25]. The possibility of the selective production of propylene by introducing tin into the H-ZSM-5 zeolite was shown in [25], where tetrapropyl ammonium hydroxide (TPHA) was used as the structure-forming agent, the selectivity to propylene was 36%, and the selectivity toward ethylene fell to 2.3%. The increase in propylene selectivity was attributed to a drop in the acidity of active sites, resulting in reduced accumulation of heavy hydrocarbons and thus an increase in the content of propylene.

Increasing the content of ethylene in the reaction medium is a difficult task associated with ensuring fairly high activity and the need to quickly remove the ethylene that forms in order to prevent further growth of the carbon chain. Introducing transition metals into the catalyst can raise the yield of ethylene. The synthesis of SAPO-34 zeotype modified with silver was described in [26] (see Table 2). The inclusion of silver raised the total acidity of the sample from 1.8 to 2.2 mmol/g, which elevated the selectivity toward ethylene from 40 to 50%.

Developing ways of synthesizing zeolites and zeotypes that allow us to vary the number and strength of acid sites is of considerable interest, due to the possibility of regulating the activity and stability of catalysts. Ways of synthesizing zeolites of the SAPO-34 type with low contents of silicon (see Table 2) via recrystallization of the initial SAPO-34 zeolite silicon were developed in [27]. The Si of the original zeolite matrix goes into a solution with subsequent secondary growth, while the Si : Al ratio falls from 0.7 to 0.28. There is also partial migration of phosphorus and aluminum during secondary crystallization, which helps lower the zeolite's acidity from 0.3 to 0.2 mol/g. The above structural changes were noted by the authors of [27] as the reason for the increase in the selectivity of the synthesized samples toward ethylene (from 27–30 to 35–37%).

EFFECT OF PROCESS CONDITIONS

The partial pressure of methanol and its specific mass rate have a considerable effect on the selectivity of methanol conversion into hydrocarbons. [28, 29]. The positive effect of a drop in the partial pressure of methanol on an increase in the selectivity of the process toward ethylene was shown using the example of zeolites and zeotypes SAPO-34 [28], SSZ-13 [29], and SSZ-39 [28] with virtually the same volume of micropores (0.27–0.28 cm^3/g) and total numbers of acid sites of 0.55, 0.92, and 0.83 mmol/g, respectively. The mass flow rate of methanol was 76–80 $kg_{Me}/(kg_{cat}$ h), while the temperature of 400°C remained constant. Lowering the partial pressure of methanol from 30 to 1–2 kPa thus raised the selectivity toward ethylene from 20–25 to 30–35%, while the selectivity for propylene fell from 40–42 to 30–35%. The effect of temperature has also been extensively studied for traditional zeolites and zeotypes [30]. Raising the temperature in the range of 400–480°C enhances the selectivity of the process toward ethylene, which can be explained by the substantial contribution from secondary reactions of the destruction of substituted aromatic compounds.

MODIFYING INDUSTRIAL CATALYSTS

Steam modification of zeolites is a well-known and well-proven method that allows both to decrease the number of acid sites and to increase the surface area of mesopores as a result of partial hydrolysis of the zeolite surface. However, this modification method is still in the focus of researchers. So, in [31] the study of the issues of steam modification of the SAPO-34 zeotype is presented, the possibility of a controlled decrease in the number of active sites is shown with varying the time of steam treatment. Testing of the steam modified SAPO-34 zeotypes showed a decrease in their activity in proportion to the time of steaming, while the ratio of ethylene to propylene remained equal to 1 : 1.

Modification of industrial samples of zeolites in order to increase the yield of ethylene and propylene with various metals and non-metals remains an urgent task, the solution of which has been devoted to a large number of works [32–34]. So, in the article [32] modification of the industrial sample of zeolite H-ZSM-5 (Zeolist international, Si : Al = 40) zinc and phosphorus by impregnation with zinc chloride solution or

phosphoric acid. The synthesized samples contained 2.2 wt % zinc and 0.92 wt % phosphorus. Testing of modified industrial samples in the reaction of catalytic methanol conversion into hydrocarbons did not reveal significant changes in the selectivity of the process for ethylene and propylene, which amounted to 15 and 18%, respectively. In this case, the rate of deactivation of zinc-modified zeolite ZSM-5 decreased by 10–15% compared to the initial sample, which may be due to a decrease in the rate of formation of polyaromatic compounds due to the modification of acid sites.

Modification of commercial zeolite H-ZSM-5 (Tosoh Co., Japan, Si : Al = 21.5) by sequential treatment with sodium hydroxide and phosphoric acid is presented in the work [33]. Treatment with sodium hydroxide promoted the formation of mesopores, improving the transport of reagents and reaction products, and treatment with phosphoric acid contributed to a slight decrease in the acidity of active sites, as a result of which the selectivity of the process with respect to propylene was increased by 10–15% (450°C, WHSV = 3 h^{-1}). In addition, catalyst deactivation was not observed within 27 h, while for the initial zeolite, a complete loss of activity occurred at the 19th hour of operation.

In work [34] describes the creation of a layer of silicalite-1 on the surface of a commercially available sample of zeolite H-ZSM-5 (CBV3024, Si : Al = 15, Zeolist international), for which a secondary growth of silicalite-1 crystals was carried out on a zeolite sample. As a result, core-shell structures with H-ZSM-5 zeolite inside silicalite-1 with a thickness of 9.4 ± 1.1 nm were obtained. Due to the weak acidic properties of the shell - silicalite-1 - a general decrease in the acidity of the composite occurs, which helps to suppress the hydrogen transfer reaction and, as a result, leads to an increase in the selectivity of the process for olefins, which reaches 90% for propylene.

Modification of acid sites of mordenite (Hongda inc., Dalian, China) by treatment with pyridine is presented in the article [35]. Analysis of the results obtained shows that mordenite modified with pyridine gives high selectivity (>65.3%) for C_2–C_4 olefins, although the methanol conversion decreases from 100 to 54%. It is also necessary to note a decrease in the ratio of the concentration of ethylene and propylene from 4.28 to 0.8, which can be attributed to a significant change in the acidic properties of mordenite.

Olefin Formation Mechanism

A comprehensive study and discussion of the formation of the first C–C bond in the process of methanol conversion into olefins continues [36]. Using the H-SAPO-34 zeotype as an example, the pathway of the primary formation of the ketene molecule is shown [36] determined in accordance with the theory of functional electron densities. The free energy values were obtained for the stage of formation of surface methoxy groups and their subsequent interaction with carbon monoxide, the formation of which is also possible in situ during the interaction of methanol with acid sites.

The paper [37] is the study of reactions occurring in the catalytic conversion of methanol into olefins, including the cycle of the formation of aromatic compounds, the alkene cycle and the cycle of the conversion of aromatic compounds, as well as the study of the diffusion characteristics of the feedstocks, olefins and aromatic products on various acid sites in straight channels, sinusoidal channel and intersections of zeolite HZSM-5 channels. The performed calculations were based on density functional theory and molecular dynamics modeling. The results show that the aromatization process occurs predominantly at the acid sites of the intersection of the channels, where the energy barrier is significantly lower than for acid sites located in straight or sinusoidal channels. The formation of polymethylbenzenes is significantly suppressed in sinusoidal and straight channels, while the formation of olefins can occur both in the channels themselves and at the intersections of the channels with equal probabilities. Consequently, the catalytic characteristics of the H-ZSM-5 zeolite in the conversion of methanol into olefins can be controlled by purposefully changing the distribution of acid sites, which, however, is an extremely difficult practical problem.

The formation of propylene and ethylene as a result of the secondary dealkylation reactions of aromatic hydrocarbons are considered in the work [38] using zeotype SAPO-34 and methanol labeled ^{13}C with a radioactive label. The predominant formation of ethylene and propylene was established as a result of dealkylation of polymethylbenzenes. In this case, ethylene is predominantly formed as a result of dealkylation of tetramethylbenzene, while propylene is formed as a result of dealkylation of tri-, penta-, and hexamethylbenzenes.

Some theoretical aspects of the influence of doping zeotype SAPO-34 and zeolite H-ZSM-5 with zirconium are considered in the work [39]. The results of calculations performed by the method of functional density theory showed that doping with Zr zeotype SAPO-34 leads to the formation of an additional pore surface, while doping with zirconium zeolite H-ZSM-5 has little effect on the pore volume. At the same time, the total acidity decreases in both cases. Zirconium doping with H-SAPO-34 increased the activity of the latter in the conversion of methanol into olefins, while the addition of zirconium to ZSM-5 did not significantly affect the activity. A significant increase in the selectivity for ethylene in both cases can be explained by a decrease in the number of strong acid sites H-ZrAPO-34 and H-ZrZSM-5.

Table 3. The pore structure of zeolites and zeotypes and their stability during the catalytic conversion of methanol into olefins

Name	D_{max}, Å	S_{this}, % [44]	S_{prop}, % [44]	G_{max}, kg (CH_3OH)/mol (H^+) [44]
SAPO-35	3.53	28	40	0.4
SAPO-42	4.21	8	17	43.3
SAPO-56	3.73	26	28	0.3
STA-7	4.1	21	29	3.7

D_{max} is the maximum hydraulic diameter of molecules that can freely diffuse through the pore. Conditions: $T = 400°C$, WHSV = 0.35 h^{-1}.

Theoretical and practical aspects of the influence of the bulk density of distribution of acid sites of the zeotype SAPO-34 on the selectivity of the process for hydrocarbons are given in the work [40]. The absence of a significant effect of the bulk density of distribution of acid sites on the selectivity of the process with respect to olefins was shown. It was found that dehydrocyclization reactions are subject to stronger diffusion restrictions than the reactions of methylation of olefins, dealkylation of aromatic hydrocarbons, and hydrogenation with hydrogen transfer.

Deactivation of Catalysts

The study of the issues of deactivation of zeolites and zeotypes remains a demanded task of modern catalysis, in connection with which the number of works in this area remains constantly high [41–43]. So, the issues of the mechanism of deactivation of the zeotype H-SAPO-34 are considered in the work [42]. It has been shown that the deactivation of the zeolite is closely related to the amount, size and location of the carbon residue formed in the pores and cells of the zeotype. The inhomogeneous spatial distribution of the carbon residue, in particular the predominant formation of the carbon residue at the intersection of the pores, leads to a significant decrease in the available acid sites and, as a consequence, to the deactivation of the catalyst in the presence of active sites free from the carbon residue. An increase in the apparent activation energy of diffusion from 6 to 8 kJ/mol for ethylene with an increase in the amount of carbon residue from 0 to 9 wt% was shown, which is a possible reason for a decrease in the selectivity of the process with respect to ethylene during the deactivation of zeolite.

Mathematical modeling of diffusion processes occurring in the SAPO-34 zeotype before and after decontamination is given in the work [43]. A two-fold increase in the activation energy of diffusion processes for ethylene, propylene, *iso*-butene and *trance*-2-butene in the case of the presence of a carbon residue in the pores of the zeotype. The change in the selectivity for olefins during the deactivation of SAPO-34 can be attributed to the effect of the change in mass transfer through the pore windows of the zeotype. Also, the deactivation of SAPO-34 zeotype correlates with the adsorption of carbon particles in the pores of the zeolite, and not with the dynamic concentration of free methoxyl groups, which mainly affect the selectivity of olefin formation.

The authors [41] considered the use of preliminary deactivation of SAPO-34 zeotype with butene-1 for the uniform formation of carbon deposits over the entire surface of the catalyst to produce a positive effect both on the possibility of long-term use of the catalyst and the process selectivity to ethylene, which increased from 40 to 50% due to a decrease in the process selectivity to hydrocarbons with more than five carbon atoms. However, it should be noted that the unmodified catalyst sample also showed a selectivity of 50% at the final stage of operation. A similar approach to regulating the activity and selectivity of catalytic systems can be implemented in practice only if a fluidized bed tray with a catalyst regenerator is used. At the same time, a variable composition of hydrocarbons will always be observed in fozed-bed reactors to the gradual deactivation of the catalyst bed.

The topology of zeolites and zeotypes has a decisive influence on the process of their deactivation [44]. Study of zeotypes SAPO-35, SAPO-42, SAPO-56, STA-7 (Table 3) showed that an increase in the size of micropores contributes to a significant increase in the maximum possible amount of converted methanol. However, an increase in pore size also contributes to an increase in the yield of heavy, including aromatic, hydrocarbons, which in turn significantly reduces the selectivity of the process for ethylene and propylene.

Technological implementation of the process

Since the early 2000s [45], the Institute of Chemical Physics of Dalian, together with the Chinese Petroleum and Chemical Corporation, worked on the technological feasibility of industrial processes of methanol conversion into olefins and to launch the first semi-industrial unit in China with a capacity of 16000 t of processed methanol per year [46] in 2006. After the successful completion of industrial tests, Shenhua Group (China) licensed and built the first plant for the production of polyethylene and polypropylene with a capacity of 0.6 million t/yr through the

stages of coal gasification, methanol synthesis, ethylene and propylene production. In 2009, there was significant progress in the industrial implementation of technology for the catalytic conversion of methanol into olefins [47]. 26 production sites licensed in the People's Republic of China [47] with a capacity of 14 million t/yr for ethylene and propylene [47] and commissioned 14 enterprises with a total capacity of 7.67 million t/yr for ethylene and propylene. The unit capacity of the existing plants was 0.6 and 0.33 thousand t/yr for ethylene and propylene, respectively. The established production facilities include a full cycle of coal processing, consisting of gasification units for synthesis gas production, units for methanol production, for the synthesis of ethylene and propylene and their purification, as well as units for the production of polyethylene and polypropylene. At the same time, the total productivity of olefins production plants in China exceeded 21 million t/yr for ethylene and propylene. The basis of the stage for obtaining olefins was a catalytic lift reactor with a fluidized bed, the period of catalyst contact is 2–3 s, and the time the catalyst resides in the reactor is no more than 60 min. The ratio of height to the diameter of the fluidized bed zone is 0.3, the diameter is 11 m, and the height of the fluidized zone is about 3–3.5 m. The familiar SAPO-34 zeotype is used as a catalyst. Each industrial site produces its own catalysts for the conversion of methanol to olefins and synthesis gas to methanol. The technological modernization of processes is proceeding in parallel with the construction of new enterprises, based on the operating experience of production facilities already launched (Fig. 1). At the initial plants for the production of 1 t of a mixture of ethylene and propylene, 2.97 t of methanol were required (see Fig. 1a), while the amount of methanol required for the production of 1 t of a mixture of ethylene and propylene was reduced to 2.67 t in the second series of units (see Fig. 1b) by adding a heavy olefin cracking stage. In the last technological variant, the required amount of methanol for the production of 1 t of a mixture of ethylene and propylene was reduced to 2.64 t by using a more efficient catalyst and increasing the conversion of the reactants [47].

Results from the industrial operation of installations were presented in [47], but the data on the possibility of producing 590000 t/yr of ethylene and 550000 t of propylene from 1.8 million t/yr of methyl alcohol raise doubts, due to the stoichiometric impossibility of obtaining such a quantity of hydrocarbons. Despite the above disadvantages, however, one cannot fail to note the colossal work of Chinese science and industry in the practical implementation of the catalytic conversion of methanol into olefins.

There are also some papers worthy of special note on determining the optimum operation modes of fluidized-bed reactors for the conversion of methanol into olefins [48, 49].

An industrial reactor with a capacity of 14000 t of CH_3OH per year using a fluidized bed of catalyst 8.5 m high, a reaction zone diameter of 1.25 m, and a reaction zone height of 1.84 m was described in [49]. The installation was simulated using a physical model of the reactor and the kinetic dependences of the formation of methane, ethylene, propylene, ethane, propane, carbon, and the C_4 and C_5 fractions of hydrocarbons. At the same time, the results from simulation differed by 8–10% from those obtained at the industrial plant, while earlier models that ignored the formation of a carbon residue on the zeolite surfaces differed from the results of the industrial plant's operation by 15–20%. The resulting mathematical models were used to optimize the operation of industrial plants for the production of olefins.

A new lift reactor for the conversion of methanol to olefins, in which two parallel reaction zones were created by introducing a stack into the column bed, was therefore described in [48]. A comparison of the new reactor and the traditional single-zone reactor showed that introducing a stack can greatly increase the velocity of the gas while simultaneously creating a central upward flow of the catalyst and a downward radial flow. It was found that around 80% of the gas flow from the supply pipe flows upward, while the rest participates in internal circulation. Reducing the time of contact to 0.5–1 s, we can increase the selectivity of the process toward ethylene by 10–15%.

Another option for the technological implementation of the process of catalytic methanol conversion into olefins is to use membrane reactors [50]. A membrane reactor allows reaction products to be withdrawn directly from the reaction zone, so a considerable increase in the selectivity toward light olefins is possible. The main problem of such a technical implementation of catalytic methanol conversion into olefins is obtaining stable catalytic membranes. The synthesis of the catalytic membrane of H-ZSM-5 zeolite by the secondary growth method was described in [50]. Zeolite crystals were deposited on a silicon oxide substrate with secondary crystals grown on them under conditions of hydrothermal synthesis. The selectivity of methanol-to-propylene conversion was 50%, while the selectivity toward ethylene was only 10–12%.

Possible upgrading for the technology of coal conversion into polypropylene and polyethylene through the methanol and olefin synthesis stages was analyzed in [51]. It is noted that the current process for converting syngas into olefins suffers from inefficient use of hydrogen, the limited olefin production in the process, and low energy efficiency. One way of solving this problem could be to use of a new technological route for the production of olefins by effectively combining the production of synthesis gas and a chemically closed combustion cycle of pulverized coke to effectively maintain a 2 : 1 ratio of hydrogen to carbon in

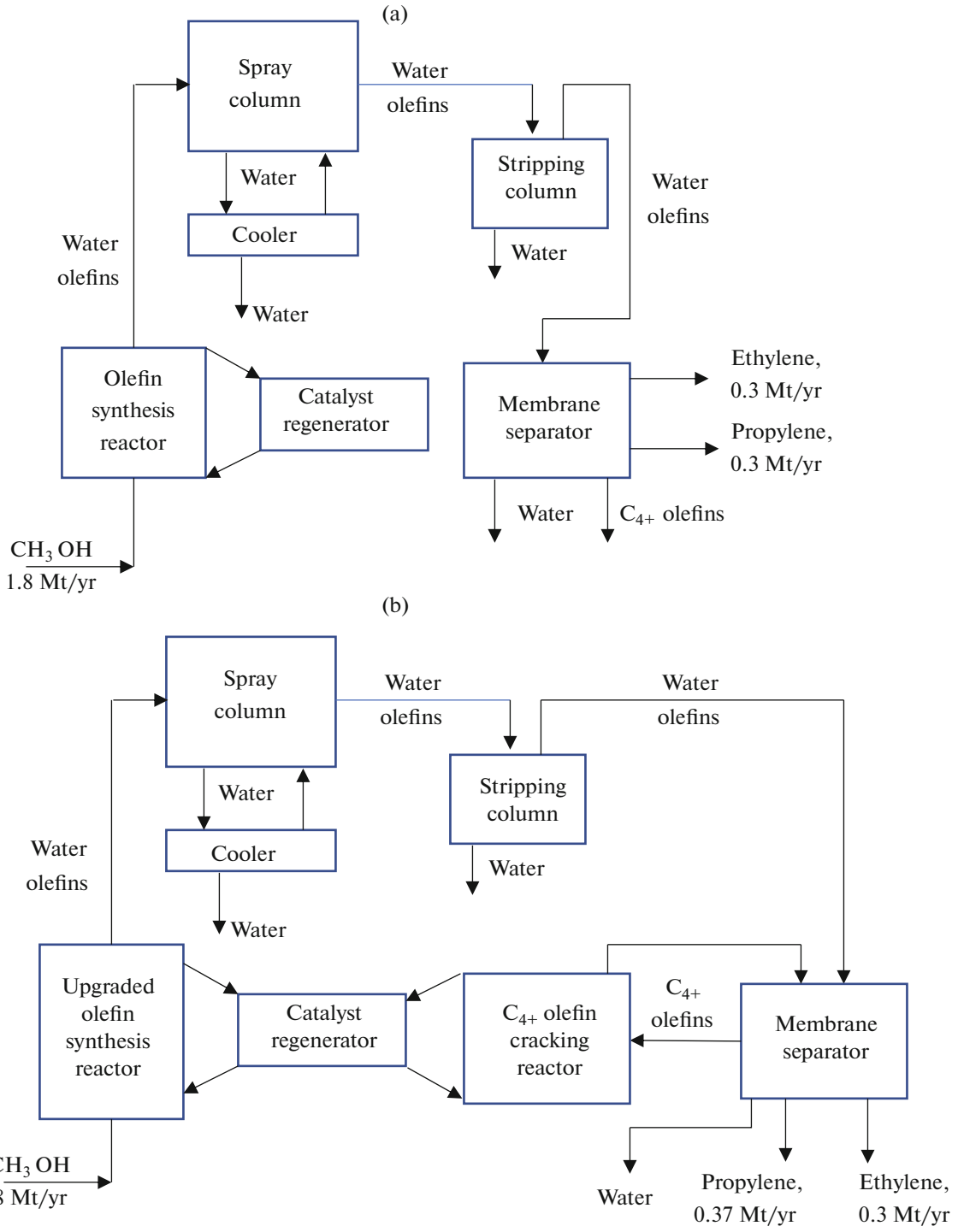

Fig. 1. (a) Initial technological scheme; (b) enhanced technological scheme for producing ethylene and propylene [47].

the synthesis gas. Features of the possible integration of a closed combustion cycle of coal with the partial recirculation and removal of carbon dioxide were considered in order to ensure acceptable environmental friendliness of the process. Results from modeling the integration of the closed combustion cycle of coal into the industrial synthesis of olefin confirmed the competitiveness of this process, showing that its hydrogen efficiency and exergy efficiency can be increased to 43 and 60%, respectively, compared to 29 and 52% for the technology now in use. The production capacity for olefins can also be increased from 0.6 to 0.9 million t/yr, due to the additional consumption of economical pulverized coal in the amount of 0.43 million t/yr. How-

ever, it should be noted that the total capital investment in the new process has risen by 21%, relative to the current cost of coal processing plants for the production of polyethylene and polypropylene.

Considerable attention has also been given to individual parts of industrial plants for the production of olefins [52–54]. The operation of an industrial high-pressure microcyclone unit used for the separation of the water–organic liquid obtained during the synthesis of olefins was studied in [52]. The efficiency of the microcyclone plant was 90% with a capacity of the incoming mixture of 282 m^3/h and a total hydraulic resistance of 0.31 MPa. Microcyclones for the separation of catalyst particles carried away by steam from the olefin synthesis reactor were also studied in [54]. A unit that included 300 mini-cyclones was created on the basis of a group of mini-hydrocyclones of parallel configuration. Experiments showed that the efficiency of separating catalyst particles 1.6 μm in size was 79.4%.

The optimization of energy costs in the conversion of methanol into olefins with a heat pump was considered in [53]. It was proposed that the output stream of the vapor phase of olefins be compressed with the temperature of the stream rising to 155°C. It would then be directed to a methanol evaporator. The saved energy would recoup the cost of the compressor in around a year. The low-pressure steam could also be used in an ammonia absorption refrigeration plant, which would cover the cooling needs of an olefin plant.

The possibility of introducing a new technology of absorption for the stage of separating synthesized olefins was considered in [55]. Wison Engineering (United States) proposed a new absorption-based olefin separation section to replace the traditional cryogenic unit. A pinch analysis showed that when fully integrated, the use of hot and cold power supplies was virtually identical for both configurations with differences of less than 1 MW for a total power supply of 60 MW. An analysis of the generated entropy showed that the irreversibility in the absorption configuration is less than in the cryogenic configuration, with relative differences of up to 20%. Analysis of the sensitivity of the sections to changes in the content of light fractions in the feed showed that the absorption unit is more sensitive to changes in the concentrations of light hydrocarbons and hydrogen in the stream than the cryogenic unit. The total capital investment for the absorption unit was estimated at USD $41 million, 13.7% below that of the cryogenic unit when it comes to low light hydrocarbons. Even with high contents of light hydrocarbons, the difference compared to a cryogenic unit is USD $10 million, which is 3.5% less than the base cost of a cryogenic unit. The main differences in capital costs are in the cost of distillation columns and compressors for refrigeration sections. The difference between the operating costs of both configurations for high light ends is less than USD $0.2 million.

Another option for upgrading the stage of olefin separation is to use a dividing wall rectification column [56]. A pilot column with a diameter of 0.8 m, specially designed for the separation of olefins, was investigated. Studies have shown that energy savings of 30% over existing technology can be achieved, and the column can also be used to separate mixtures with low olefin contents.

The full life cycle of the conversion of coal into polyethylene and polypropylene through the stages of olefin formation has been considered in a fairly large number of published works, based on the example of industrial enterprises of the People's Republic of China [57–60]. It was noted that the primary conversion of coal into methanol consumes large amounts of water (up to 25 t per ton of formed methanol) and energy (up to 120 GJ per ton of produced methanol) [57]. The primary synthesis of methanol from coal in this case results in the emission of 8 t of carbon dioxide per ton of generated methanol. The conversion of methanol into olefins is accompanied by the consumption of around 5 t of water per ton of formed olefins and 20 GJ of energy per ton of produced olefins. However, the authors did not consider problems of the partial recovery of water and energy during the conversion of coal into polyethylene and polypropylene through the stages of olefin formation, making the obtained figures extremely overestimated. It should be noted that the theoretically justified amount of water for the production of 1 t of methanol through the stage of obtaining synthesis gas from coal is 3 t, while the stage of obtaining olefins almost completely recvers the water spent in that of obtaining synthesis gas.

The detailed estimation of economic aspects in the production of olefins was presented in [58], where the authors considered twenty main technological options for the production of olefins. The possibility of reducing the total production costs by 23% through raising the scale of olefin production from 100000 to 1 million t/yr was established. At the same time, the value of 300000 t of olefins per year can be recognized as the minimum justified productivity of an enterprise for the synthesis of olefins. Lower prices for raw materials have a positive effect on the overall return on production and profitability. Coal and natural gas are now the preferred resources for the production of olefins. Lower prices for biofuels and hydrogen can reduce overall production costs for renewables, but these measures are not enough to compete successfully with coal and natural gas technologies. This means renewable energy sources cannot completely replace fossil resources for olefin production in the short term. Government financial support and preferential taxation policies are required to ensure the competitiveness of olefin production using renewable raw materials [58].

A fairly in-depth analysis of the industrial production of olefins in the People's Republic of China was

presented in [59, 60]. The authors of [59] showed that raw material costs are most important in the total cost of olefin production. The model of the industrial production of olefins developed in China reflects the dynamics of oil and coal prices to achieve economic and environmental security in China. The optimum configuration of China's facilities for the production of olefins in the period 2016 to 2035 has been analyzed under four different scenarios of changes in oil and coal prices. In the first (baseline) scenario, a constant price for resources was assumed throughout the period of study. In the second, the price of crude oil will rise as predicted by OPEC in 2016, while the price of coal will remain the same as in the initial period of study. In the third, the price of coal will rise according to the forecast of the World Energy Agency WEA (2015) while the price of crude oil remains constant. In the fourth (most realistic) scenario, oil and coal prices will rise in line with OPEC and WEA forecasts. The production of olefins from coal will have important advantages if the economic situation develops according to the first and second scenarios. The capacity for the production of olefins from coal can be expanded if the economic situation follows the third and fourth scenarios. The possibility of controlling emissions of carbon dioxide by introducing systems for its capture and processing is also being investigated. Modeling results show that the introduction of such systems for capturing carbon dioxide would greatly limit the possible increase in the capacity of enterprises for the conversion of coal into olefins. In all four scenarios, however, olefins from coal would account for at least 13% of China's gross olefin production after introducing regulations for capturing and storing carbon. Calculations also show that an economically viable implementation of carbon dioxide treatment and storage systems would be possible if the price of crude oil is above USD $66 per barrel. It should be noted that the introduction of systems for the recovery and storage of carbon dioxide could reduce carbon dioxide emissions by 63–74%. The production of olefins from coal in China remains competitive even after the introduction of a carbon tax of $20/t in 2021 [60].

The possible use of technological processes for the production of polyethylene through stages of methanol synthesis and the production of olefins as a way of utilizing carbon dioxide from the flue gases of metal processing industries was analyzed in [61]. The minimum estimated selling prices for ethylene were USD $2030/t when using only hydrogen from coke oven gas and USD $1064/t when coke oven gas was used as feedstock. Both obtained values were higher than the current minimum selling price for ethylene (USD $720/t of ethylene obtained from oil). An economic analysis of the results shows that the proposed ways of processing carbon dioxide are not economically feasible under current conditions.

ENVIRONMENTAL ASPECTS OF THE TECHNOLOGICAL IMPLEMENTATION OF THE OLEFIN PRODUCTION

The growing coal-to-olefin capacity contributes to increased environmental pollution, mainly in China [62]. According to the plan for developing olefin production in China [63], carbon dioxide emissions will reach 189.43 million t in 2020 and 314.11 million t by 2030. The number of works aimed at studying the life cycle of olefin production in order to reduce the negative impact on the environment is therefore growing [62]. One way of solving the above problem is to expand the use of associated petroleum gases as an additive to coal at the stage of obtaining synthesis gas and in other ways. Results show that producing olefins from coal generally has a greater environmental impact than producing them from oil or natural gas. The resulting carcinogens are the main factors affecting the environment. Converting coal to methanol using associated gas from oil fields or natural gas reduces the potential environmental impact by as much as 50%, due to a 73% reduction in coal consumption.

To reduce carbon dioxide emissions, we can also use processes for the production of olefins via the conversion of carbon dioxide into methanol or bioethanol into olefins, which would help reduce carbon dioxide emissions by 500 million t/yr [64]. The research results [64] emphasize the key role of the Chinese Communist Party in reducing carbon dioxide emissions by raising the average technological level of chemical production and preparing for the transition to low-carbon processes in the Chinese chemical industry.

STATE-OF-THE-ART AND PROSPECTS IN DEVELOPING THE CATALYTIC CONVERSION OF METHANOL INTO OLEFINS IN RUSSIA

In Russia, the leading position in the field of research on the catalytic conversion of methanol into olefins is traditionally held by the Russian Academy of Sciences' Topchiev Institute of Petrochemical Synthesis. Over the past five years, it has done a considerable amount of research on developing catalysts for the production of olefins based on zeolites and zeotypes H-ZSM-5 and SAPO-18, modified with metals Zn, Fe, Mg, Pd (Table 4) [65–70].

Among the studied catalysts, special note should be taken of the SAPO-18 zeotype, which displayed a high selectivity of 83% toward olefins and a resistance to deactivation comparable to that of SAPO-34 [69], making it a promising material for industrial use. Bifunctional catalyst Pd-Zn-HZSM-5/Al_2O_3 developed in [68] is of special interest. It allows the simultaneous synthesis of methanol from synthesis gas and

Table 4. Catalysts for the synthesis of olefins from methanol

Sample	Composition	Si : Me	T, °C	WHSV, h^{-1}	S_{et}, %	S_{prop}, %	Reference
Mg-ZSM-5/Al_2O_3	Mg, 1 wt % ZSM-5, 76.5 wt % Al_2O_3, 32.5 wt %	37	450	6.3	14	36	[65, 67]
Fe-ZSM-5	Fe, 2.2 wt %, ZSM-5, 97.8 wt %	—	490	1	19	54	[66]
SAPO-18	SAPO-18, 100 wt %	—	400	2	45	38	[69]
H-ZSM-5/halloyside	ZSM-5, 77 wt %, Halloyside, 33 wt %	37	320	1	15	30	[70]

the synthesis of olefins and heavier hydrocarbons, while the selectivity toward ethylene and propylene is 8 and 11%, respectively (H_2 : CO: N_2 : DME = 86 : 3 : 11 : 1; P = 100 atm, T = 380°C).

CONCLUSIONS

Based on a review of the literature, we can reach conclusions on both ways of synthesizing zeolites and zeotypes and modifying them to increase the yield of olefins and the service life of catalysts. The development of metal-modified zeolites and zeotypes can make an important contribution to improving the technological parameters of the catalytic conversion of methanol into olefins. It should also be noted that zeotype SAPO-34 is the main catalyst currently used in industrial plants for producing olefins from methanol. Industrial plants for the synthesis of olefins from methanol are based on using a fluidized bed tray with a catalyst regenerator, which ensures the consistency of the composition of the resulting olefins and the ability to control the productivity of the units in a wide range of values. The decribed feasibility studies for the industrial production of olefins from coal demonstrate the possibility of the widespread use of this technology and its economic feasibility. We can also use these technological solutions economically, even if we have to create installations for the capture and utilization of carbon dioxide. At the same time, the environmental aspects of using the technology for producing olefins through the stages of coal gasification and methanol synthesis are of concern to the wide strata of society. At the same time, the main way of solving possible environmental problems is to continue developing the scientific and technical level of production.

In Russia, the technology for producing olefins from methanol can be industrialized using both natural gas and such solid fuels as coal, brown coal, peat, and biomass. The fundamental factors that determine the feasibility of introducing the above technology are in this case the specific economic conditions, the need for olefins, and the possibility of using both indigenous and foreign technological solutions.

FUNDING

This work was supported by the Russian Foundation for Basic Research (project no. 20-38-51001), NTU Sirius, OAO Russian Railways, and the Educational Foundation "Talent and Success."

REFERENCES

1. US Patent 4499327B1, 1992.
2. Lewis, J.M.O., *Stud. Surf. Sci. Catal.,* 1988, vol. 38, pp. 199–207. https://doi.org/10.1016/S0167-2991(09)60656-X
3. Vora, B.V., Marker, T.L., Barger, P.T., Nilsen, H.R., Kvisle, S., and Fuglerud, T., *Stud. Surf. Sci. Catal.,* 1997, vol. 107, pp. 87–98. https://doi.org/10.1016/S0167-2991(97)80321-7
4. Barger, P.T., Vora, B.V., Pujadó, P.R., and Chen, Q., *Stud. Surf. Sci. Catal.,* 2003, vol. 145, pp. 109–114. https://doi.org/10.1016/S0167-2991(03)80173-8
5. Chen, J.Q., Bozzano, A., Glover, B., Fuglerud, T., and Kvisle, S., *Catal. Today,* 2005, vol. 106, no. 1, pp. 103–107.
6. Chen, J.Q., Vora, B.V., Pujadó, P.R., Gronvold, Fuglerud, T., and Kvisle, S., and *Stud. Surf. Sci. Catal.,* 2004, vol. 147, pp. 1–6. https://doi.org/10.1016/S0167-2991(04)80018-1
7. MTO complex planned for Nigeria, *Focus Catal.,* 2002, vol. 2002, no. 12. https://doi.org/10.1016/S1351-4180(02)01240-0
8. Technip to deliver Belgian demo MTO unit, *Pump Ind. Anal.,* 2006, vol. 2006, no. 2, pp. 3–4. https://doi.org/10.1016/S1359-6128(06)71248-4
9. Gogate, M.R., *Pet. Sci. Technol.,* 2019, vol. 37, no. 5, pp. 603–610. https://doi.org/10.1080/10916466.2018.1558248
10. Sun, C., Wang, Y., Zhao, A., Wang, X., Wang, C., Zhang, X., Wang, Z., Zhao, J., and Zhao, T., *Appl. Catal., A,* 2020, vol. 589, https://doi.org/10.1016/j.apcata.2019.117314
11. Jiang, X., Su, X., Bai, X., Li, Y., Yang, L., Zhang, K., Zhang, Y., Liu, Y., and Wu, W., *Microporous Mesoporous Mater.,* 2018, vol. 263, pp. 243–250. https://doi.org/10.1016/j.micromeso.2017.12.029
12. Losch, P., Pinar, A.B., Willinger, M.G., Soukup, K., Chavan, S., Vincent, B., Pale, P., and Louis, B.,

J. Catal., 2017, vol. 345, pp. 11–23. https://doi.org/10.1016/j.jcat.2016.11.005

13. Huang, F., Cao, J., Wang, L., Wang, X., and Liu, F., *Chem. Eng. J.,* 2020, vol. 380. https://doi.org/10.1016/j.cej.2019.122626
14. Mousavi, S.H., Fatemi, S., and Razavian, M., *Particuology,* 2018, vol. 37, pp. 43–53. https://doi.org/10.1016/j.partic.2017.06.004
15. Nasser, G.A., Muraza, O., Nishitoba, T., Malaibari, Z., Al-Shammari, T.K., and Yokoi, T., *Microporous Mesoporous Mater.,* 2019, vol. 274, pp. 277–285. https://doi.org/10.1016/j.micromeso.2018.07.020
16. Yalcin, B.K. and Ipek, B., *Appl. Catal., A,* 2021, vol. 610. https://doi.org/10.1016/j.apcata.2020.117915
17. Han, Z., Zhou, F., Zhao, J., Liu, Y., Ma, H., and Wu, G., *Microporous Mesoporous Mater.,* 2020, vol. 302. https://doi.org/10.1016/j.micromeso.2020.110194
18. Han, Z., Zhou, F., Liu, Y., Qiao, K., Ma, H., Yu, L., and Wu, G., *J. Taiwan Inst. Chem. Eng.,* 2019, vol. 103, pp. 149–159. https://doi.org/10.1016/j.jtice.2019.07.005
19. Park, S., Sato, G., Nishitoba, T., Kondo, J.N., and Yokoi, T., *Catal. Today,* 2020, vol. 352, pp. 175–182. https://doi.org/10.1016/j.cattod.2019.12.008
20. Huang, H., Yu, M., Zhang, Q., and Li, C., *Microporous Mesoporous Mater.,* 2020, vol. 295. https://doi.org/10.1016/j.micromeso.2019.109971
21. Chae, H.-J., Park, S.S., Shin, Y.H., and Park, M.B., *Microporous Mesoporous Mater.,* 2018, vol. 259, pp. 60–66. https://doi.org/10.1016/j.micromeso.2017.09.035
22. Tsunoji, N., Osuga, R., Yasumoto, M., and Yokoi, T., *Appl. Catal., A,* 2021, vol. 620. https://doi.org/10.1016/j.apcata.2021.118176
23. Azarhoosh, M.J., Halladj, R., Askari, S., and Aghaeinejad-Meybodi, A., *Ultrason. Sonochem.,* 2019, vol. 58. https://doi.org/10.1016/j.ultsonch.2019.104646
24. Sadeghpour, P. and Haghighi, M., *Adv. Powder Technol.,* 2018, vol. 29, no. 5, pp. 1175–1188. https://doi.org/10.1016/j.apt.2018.02.009
25. Xue, Y., Li, J., Wang, P., Cui, X., Zheng, H., Niu, Y., Dong, M., Qin, Z., Wang, J., and Fan, W., *Appl. Catal., B*, 2021, vol. 280. https://doi.org/10.1016/j.apcatb.2020.119391
26. Hashemi, F., Taghizadeh, M., and Rami, M.D., *Microporous Mesoporous Mater.,* 2020, vol. 295. https://doi.org/10.1016/j.micromeso.2019.109970
27. Wang, X., Li, Z., Gong, F., Ma, M., and Zhu, Y., *Mol. Catal.,* 2021, vol. 499. https://doi.org/10.1016/j.mcat.2020.111312
28. Shi, Z. and Bhan, A., *J. Catal.,* 2021, vol. 395, pp. 266–272. https://doi.org/10.1016/j.jcat.2021.01.015
29. Hwang, A., Kumar, M., Rimer, J.D., and Bhan, A., *J. Catal.,* 2017, vol. 346, pp. 154–160. https://doi.org/10.1016/j.jcat.2016.12.003
30. Ebadzadeh, E., Khademi, M.H., and Beheshti, M., *Chem. Eng. J.,* 2021, vol. 405. https://doi.org/10.1016/j.cej.2020.126605
31. Minova, I.B., Barrow, N.S., Sauerwein, A.C., Naden, A.B., Cordes, D.B., Slawin, A.M.Z., Schuyten, S.J., and Wright, P.A., *J. Catal.,* 2021, vol. 395, pp. 425–444. https://doi.org/10.1016/j.jcat.2021.01.012
32. Valecillos, J., Epelde, E., Albo, J., Aguayo, A.T., Bilbao, J., and Castaño, P., *Catal. Today,* 2020, vol. 348, pp. 243–256. https://doi.org/10.1016/j.cattod.2019.07.059
33. Tanaka, S., Fukui, R., Kosaka, A., and Nishiyama, N., *Mater. Res. Bull.,* 2020, vol. 130. https://doi.org/10.1016/j.materresbull.2020.110958
34. Suttipat, D., Saenluang, K., Wannapakdee, W., Dugkhuntod, P., Ketkaew, M., Pornsetmetakul, P., and Wattanakit, C., *Fuel,* 2021, vol. 286, part 1. https://doi.org/10.1016/j.fuel.2020.119306
35. He, T., Hou, G., Li, J., Liu, X., Xu, S., Han, X., and Bao, X., *J. Energy Chem.,* 2017, vol. 26, no. 3, pp. 354–358. https://doi.org/10.1016/j.jechem.2017.02.004
36. Zang, K., Zhang, W., Huang, J., Feng, P., and Ding, J., *Chem. Phys. Lett.,* 2019, vol. 737. https://doi.org/10.1016/j.cplett.2019.136844
37. Wang, S., Li, Z., Qin, Z., Dong, M., Li, J., Fan, W., and Wang, J., *Chin J. Catal.,* 2021, vol. 42, no. 7, pp. 1126–1136. https://doi.org/10.1016/S1872-2067(20)63732-9
38. Hwang, A., Johnson, B.A., and Bhan, A., *J. Catal.,* 2019, vol. 369, pp. 86–94. https://doi.org/10.1016/j.jcat.2018.10.022
39. Li, D., Xing, B., Wang, B., and Li, R., *Fuel Process. Technol.,* 2020, vol. 199. https://doi.org/10.1016/j.fuproc.2019.106302
40. Hwang, A., Le, T.T., Shi, Z., Dai, H., Rimer, J.D., and Bhan, A., *J. Catal.,* 2019, vol. 369, pp. 122–132. https://doi.org/10.1016/j.jcat.2018.10.031
41. Zhou, J., Zhi, Y., Zhang, J., Liu, Z., Zhang, T., He, Y., Zheng, A., Ye, M., Wei, Y., and Liu, Z., *J. Catal.,* 2019, vol. 377, pp. 153–162. https://doi.org/10.1016/j.jcat.2019.06.014
42. Gao, S., Xu, S., Wei, Y., Qiao, Q., Xu, Z., Wu, X., Zhang, M., He, Y., Xu, S., and Liu, Z., *J. Catal.,* 2018, vol. 367, pp. 306–314. https://doi.org/10.1016/j.jcat.2018.09.010
43. Lo, B.T.W., Ye, L., Chang, G.G.Z., Purchase, K., Day, S., Tang, C.C., Mei, D., and Tsang, S.C.E., *Appl. Catal., B*, 2018, vol. 237, pp. 245–250. https://doi.org/10.1016/j.apcatb.2018.05.090
44. Pinilla-Herrero, I., Olsbye, U., Márquez-Álvarez, C., and Sastre, E., *J. Catal.,* 2017, vol. 352, pp. 191–207. https://doi.org/10.1016/j.jcat.2017.05.008
45. Xu, X., Liu, Y., Zhang, F., Di, W., and Zhang, Y., *Catal. Today,* 2017, vol. 298, pp. 61–68. https://doi.org/10.1016/j.cattod.2017.05.070
46. Chen, J.-M., Yu, B., and Wei, Y.-M., *Appl. Energy,* 2018, vol. 224, pp. 160–174. https://doi.org/10.1016/j.apenergy.2018.04.051
47. Ye, M., Tian, P., and Liu, Z., *Engineering,* 2021, vol. 7, no. 1, pp. 17–21. https://doi.org/10.1016/j.eng.2020.12.001

48. Zhang, C., Wang, F., Lu, B., Wang, W., Liu, M., and Lu, C., *Powder Technol.,* 2020, vol. 372, pp. 336–350. https://doi.org/10.1016/j.powtec.2020.06.010
49. Zhang, J., Lu, B., Chen, F., Li, H., Ye, M., and Wang, W., *Chem. Eng. Sci.,* 2018, vol. 189, pp. 212–220. https://doi.org/10.1016/j.ces.2018.05.056
50. Tanizume, S., Maehara, S., Ishii, K., Onoki, T., Okuno, T., Tawarayama, H., Ishikawa, S., and Nomura, M., *Sep. Purif. Technol.,* 2021, vol. 254. https://doi.org/10.1016/j.seppur.2020.117647
51. Xiang, D., Liu, S., Xiang, J., and Cao, Y., *Energy Convers. Manage.,* 2017, vol. 152, pp. 239–249. https://doi.org/10.1016/j.enconman.2017.09.053
52. Lv, W.-J., Dang, Z.-H., He, Y., Chang, Y.-L., Ma, S.-H., Liu, B., Gao, L.-X., and Ma, L., *Chem. Eng. Process.,* 2020, vol. 149. https://doi.org/10.1016/j.cep.2020.107846
53. Dimian, A.C. and Bildea, C.S., *Chem. Eng. Res. Des.,* 2018, vol. 131, pp. 41–54. https://doi.org/10.1016/j.cherd.2017.11.009
54. Lv, W.-J., Chen, J.-Q., Chang, Y.-L., Liu, H.-L., and Wang, H.-L., *Chem. Eng. Process.,* 2018, vol. 131, pp. 34–42. https://doi.org/10.1016/j.cep.2018.03.015
55. Reyniers, P.A., Vandewalle, L.A., Saerens, S., de Smedt, P., Marin, G.B., and Van Geem, K.M., *Appl. Therm. Eng.,* 2017, vol. 115, pp. 477–490. https://doi.org/10.1016/j.applthermaleng.2016.12.124
56. Ge, X., Liu, B., Yuan, X., Luio, Y., and Yu, K.-K., *Chin. J. Chem. Eng.,* 2017, vol. 25, no. 8, pp. 1069–1078. https://doi.org/10.1016/j.cjche.2017.03.018
57. Gao, D., Qiu, X., Zhang, Y., and Liu, P., *Comput. Chem. Eng.,* 2018, vol. 109, pp. 112–118. https://doi.org/10.1016/j.compchemeng.2017.11.001
58. Zhao, Z., Jiang, J., and Wang, F., *J. Energy Chem.,* 2021, vol. 56, pp. 193–202. https://doi.org/10.1016/j.jechem.2020.04.021
59. Xu, Z., Zhang, Y., Fang, C., Yu, Y., and Ma, T., *Energy Policy,* 2019, vol. 135. https://doi.org/10.1016/j.enpol.2019.111004
60. Xu, Z., Fang, C., and Ma, T., *Energy,* 2020, vol. 191. https://doi.org/10.1016/j.energy.2019.116462
61. Lee, J.-K., Shin, S., Kwak, G.-J., Lee, M.-K., Lee, I.-B., and Yoon, Y.-S., *Energy Convers. Manage.,* 2020, vol. 224. https://doi.org/10.1016/j.enconman.2020.113316
62. Ye, L., Xie, F., Hong, J., Yang, D., Ma, X., and Li, X., *Energy,* 2018, vol. 157, pp. 1015–1024. https://doi.org/10.1016/j.energy.2018.05.167
63. Shen, Q., Song, X., Mao, F., Sun, N., Wen, X., and Wei, W., *J. Environ. Sci.,* 2020, vol. 90, pp. 352–363. https://doi.org/10.1016/j.jes.2019.11.004
64. Zhao, Z., Chong, K., Jiang, J., Wilson, K., Zhang, X., and Wang, F., *Renewable Sustainable Energy Rev.,* 2018, vol. 97, pp. 580–591. https://doi.org/10.1016/j.rser.2018.08.008
65. Golubev, K.B., Batova, T.I., Kolesnichenko, N.V., and Maximov, A.L., *Catal. Commun.,* 2019, vol. 129. https://doi.org/10.1016/j.catcom.2019.105744
66. Li, Y., Su, X., Maximov, A.L., Bai, X., Wang, Y., Wang, W., Kolesnichenko, N.V., Bukina, Z.M., and Wu, W., *Russ. J. Appl. Chem.,* 2020, vol. 93, no. 1, pp. 137–148. https://doi.org/10.1134/S1070427220010152
67. Bondarenko, G.N., Rodionov, A.S., Kolesnichenko, N.V., Batova, T.I., Khivrich, E.N., and Maximov, A.L., *Catal. Lett.,* 2021, vol. 151, no. 5, pp. 1309–1319. https://doi.org/10.1007/s10562-020-03399-2
68. Maximov, A.L., Magomedova, M.V., Galanova, E.G., Afokin, M.I., and Ionin, D.A., *Fuel Process. Technol.,* 2020, vol. 199. https://doi.org/10.1016/j.fuproc.2019.106281
69. Konnov, S.V., Pavlov, V.S., and Ivanova, I.I., *Microporous Mesoporous Mater.,* 2020, vol. 300. https://doi.org/10.1016/j.micromeso.2020.110158
70. Afokin, M.I., Smirnova, E.M., Starozhitskaya, A.V., Gushchin, P.A., Glotov, A.P., and Maksimov, A.L., *Chem. Technol. Fuels Oils,* 2020, vol. 55, no. 6, pp. 682–688. https://doi.org/10.1007/s10553-020-01082-1